# Suppression of inner ear signal intensity on fluid-attenuated inversion recovery magnetic resonance imaging in cats with vestibular disease

**Stephen Everest[1]** iD **, Gabrielle Monteith[2], Luis Gaitero[2] and Francesca Samarani[2]**

## Abstract

*Objectives* Otitis media/interna (OMI) is the most common cause of peripheral vestibular disease in cats. The inner ear contains endolymph and perilymph, with perilymph being very similar in composition to cerebrospinal fluid (CSF). As a very-low-protein fluid, it would be expected that normal perilymph should suppress on fluid-attenuated inversion recovery (FLAIR) MRI sequences. Based on this, we hypothesized that MRI FLAIR sequences should provide a non-invasive way of diagnosing inflammatory/infectious diseases such as OMI in cats, something that has previously been demonstrated in humans and, more recently, in dogs.

*Methods* This was a retrospective cohort study in which 41 cats met the inclusion criteria. They were placed into one of four groups, based on presenting complaint: clinical OMI (group A); inflammatory central nervous system (CNS) disease (group B); non-inflammatory structural disease (group C); and normal brain MRI (control group; group D). Transverse T2-weighted and FLAIR MRI sequences at the level of the inner ears bilaterally were compared in each group. The inner ear was selected as a region of interest using Horos, with a FLAIR suppression ratio calculated to account for variability in signal intensity between MRIs. This FLAIR suppression ratio was then compared between groups. Statistical analyses were performed by an experienced statistician, with a general linear model used to compare mean FLAIR suppression ratio, CSF nucleated cell count and CSF protein concentration between groups.

*Results* The OMI group (group A) had significantly lower FLAIR suppression scores compared with all other groups. The CSF cell count was also significantly increased in the OMI (group A) and inflammatory CNS disease (group B) groups compared with the control group (group D).

*Conclusions and relevance* This study demonstrates the utility of MRI FLAIR sequences in diagnosing presumptive OMI in cats, similarly to in humans and dogs. This study is relevant to practicing veterinary neurologists and radiologists in interpreting MRI findings in cats with suspected OMI.

**Keywords:** FLAIR; MRI; neuroimaging; neurology; otitis; radiology; vestibular

## Introduction

Otitis media/interna (OMI) is the most common cause of vestibular disease in cats.[1] Other important differentials include idiopathic vestibular syndrome, intracranial neoplasia, middle ear polyps, feline infectious peritonitis (FIP), thiamine deficiency and intracranial empyema. Together with OMI, these conditions accounted for 95% of vestibular signs in cats in one study.[1] OMI can cause vestibular signs ipsilateral to the side of disease due to alteration of the composition of the fluid contained within

[1]Ontario Veterinary College Health Science Centre, University of Guelph, Guelph, ON, Canada
[2]Department of Clinical Studies, University of Guelph, Guelph, ON, Canada

**Corresponding author:**
Stephen Everest BSc, BVM&S, Ontario Veterinary College Health Science Centre, University of Guelph, Guelph, ON N1G 2W1, Canada
Email: everest@uoguelph.ca

the vestibule – the sensory organ responsible for vestibular input.[2]

The vestibule, as well as the cochlea – the auditory sensory organ – are contained within the inner ear. The sensory components of the inner ear are made up of two components, an outer, osseous labyrinth, and an inner, membranous labyrinth. The osseous component contains perilymph, a fluid very similar in composition to cerebrospinal fluid (CSF), and the membranous labyrinth contains endolymph.[3] The osseous labyrinth responsible for vestibular sensory input makes up the semi-circular canals through modified osseous ampullae that branch from the vestibule. The osseous ampullae are lined by the membranous ampullae. These contain the primary vestibular sensory organs, known as the cristae ampullaris, which are innervated by the vestibular nerve. These are also known as sensory hair cells due to their hair-like appearance.[3] Inflammation, and changes to the composition of the perilymph and endolymph, can therefore affect the sensory input from the vestibulocochlear nerve ipsilateral to the lesion, leading to vestibular signs.[3]

As previously noted, perilymph contained within the osseous labyrinth is very similar in composition to CSF, and actually communicates with it.[4] For this reason, the contents of the inner ear show the same hyperintensity in T2-weighted (T2W) MRI as we would expect to see when looking at normal CSF (eg, in the ventricles). In patients with no inner or middle ear pathology, it is therefore expected that the fluid contents in these organs should suppress on fluid-attenuated inversion recovery (FLAIR) MRI sequences, as seen with normal CSF.

Diagnosis of OMI can be confirmed by cytology and culture of material obtained by myringotomy, and this has been considered the gold standard for diagnosing otitis media in dogs.[5] This is a relatively invasive approach, requiring puncture of the tympanic membrane, and has resulted in deafness in some humans.[6] A less invasive approach for diagnosing OMI would be through comparison of T2W and FLAIR sequences of the inner ear. As noted above, in normal patients we would expect the same T2W hyperintensity and FLAIR suppression as would typically be seen when looking at CSF. In patients with inner ear inflammatory disease, we would expect an increase in the fluid protein concentration and cell count.[7–9] As there is communication between the CSF and perilymph, we also believe there may be decreased FLAIR suppression in cats with meningoencephalitis.

In humans, there have been numerous studies of the diagnostic utility of MRI in patients with inner ear disease.[10–12] A 2020 study by Castillo et al[13] confirmed that there was decreased suppression in FLAIR MRI sequences in the affected inner ears of dogs with OMI vs the unaffected sides. They were also shown to have reduced FLAIR suppression compared with a control group consisting of dogs with a normal brain and no evidence of vestibular disease.

For this study, we hypothesized that there would be decreased FLAIR suppression on the clinically affected side of the lesion in cats with OMI, compared with cats without clinical inner ear disease. It was also hypothesized that inner ear FLAIR suppression would be lower in cats with brain/meningeal inflammatory disease. Finally, we also hypothesized that CSF cell count and protein concentration would be negatively correlated with inner ear FLAIR suppression.

## Materials and methods

This was a retrospective cohort study. The medical records of all cats that had a brain/head MRI performed between January 2015 and November 2020 at a single academic referral center were reviewed. Cases were included if MRI included T2W and T2 FLAIR images of both inner ears, and complete clinical records were available. A total of 45 cases were identified.

All patients' medical records were reviewed, with the following data from each patient recorded by a neurology specialty intern (SE): signalment (age, sex and breed); body weight; presenting complaint; presence or absence of vestibular signs; and presumptive diagnosis. Where available, the CSF total nucleated cell count and total protein results were also recorded. Owing to the relatively small sample size, and the lack of histopathology on the vast majority of the cats in the study, there was a relatively high number of cats (5/6) with presumptive OMI diagnoses included in the study.

Patients included in the study were placed into one of four groups: cats with presumptive OMI (ie, presenting with peripheral vestibular signs, with T2 hyperintensity in the ipsilateral tympanic bulla ± contrast enhancement on MRI and no other causes for vestibular disease identified; group A); cats with inflammatory central nervous system (CNS) diseases (group B); cats with non-inflammatory, structural CNS diseases (group C); and cats with no brain abnormalities detected on MRI (control group; group D). These groups were decided by two ECVN board-certified neurologists (FS, LG) and a neurology specialty intern (SE). The negative control group (group D) included patients with idiopathic epilepsy or those with lesions identified elsewhere (eg, the vertebral column) but with no brain abnormalities noted on MRI. Criteria for inclusion in group A included cats that presented with clinical vestibular disease and had a presumptive diagnosis of OMI based on MRI findings that fitted with the neurolocalization on neurological examination. This included cats with T2W hyperintensity and contrast enhancement in the tympanic bullae and inner ear on T1-weighted (T1W) postcontrast images, with or without bulla osteolysis and changes to the surrounding musculature ipsilateral to the peripheral vestibular signs. Cats included in group B had to have evidence of pleocytosis on CSF analysis and a presumptive diagnosis of meningoencephalitis or ventriculitis based on MRI, CSF findings ± response to treatment. Cats were included in

group C if they had evidence of structural brain disease on MRI that was highly suspected to be non-inflammatory based on MRI ± CSF findings. These included various intra- and extra-axial neoplasms, infarctions and one case of porencephaly. Four cases were excluded at this stage as they either had unconfirmed diagnoses or did not fit into any of the proposed groups.

MRI performed prior to July 2016 was done with a 1.5 T MRI scanner (Signa Excite II, Software version 11.0; General Electric Medical Systems) with an eight-channel quad knee coil used for all cats. MRIs performed after July 2016 were performed with a 1.5 T MRI scanner (Signa Explorer, Software version 25.1; General Electric Medical Systems), with a small 16-channel Geometry Embracing Method coil used for all patients. Both the T2W fast spin echo (FSE) and T2W FLAIR sequences were standardized between patients, with field of view ranging from $12 \times 12$ cm to $20 \times 20$ cm, matrix from $192 \times 192$ to $320 \times 256$, and slice thickness from 3 mm to 4 mm.

Transverse T2W FSE images and T2W FLAIR images at the level of the inner ear were compared. DICOM viewing software (Horos; https://horosproject.org), was used by a neurology specialty intern to manually delineate the fluid-filled inner ears on both sides on the T2W FSE images (Figure 1). These regions of interest (ROIs) were then copied on to the corresponding T2W FLAIR images and the mean signal intensity from each was recorded. At the time of selecting these ROIs, the observer was blinded to the clinical information and final diagnosis for each cat.

To account for variation of signal intensity between images, FLAIR suppression was calculated as a ratio for each case using: FLAIR suppression = T2 – T2 FLAIR/T2. This was then compared between groups as opposed to T2W FSE and T2W FLAIR values directly, in order to normalize the results.

The FLAIR suppression ratio was compared between the ears of cats with clinical OMI suspected based on MRI findings, and the inner ears of cats in the other groups. In order for the inner ear to be considered affected, the cats had to have neurological deficits consistent with inner ear disease, with corresponding findings seen on MRI. For example, if lateralized signs were present, but the MRI showed both ears to be affected, only the side for which the cat was clinically affected was included in the affected group.

### Statistical analysis

A commercially available software (Stat 9.4; SAS Institute) was used by an experienced statistician to perform the statistical analyses. In order to compare the mean FLAIR suppression ratio, CSF nucleated cell count and CSF protein concentration between groups, a general linear regression model was used, which included the pathology groups (groups A–D) as well as sex (female intact, female spayed and male castrated) and age.
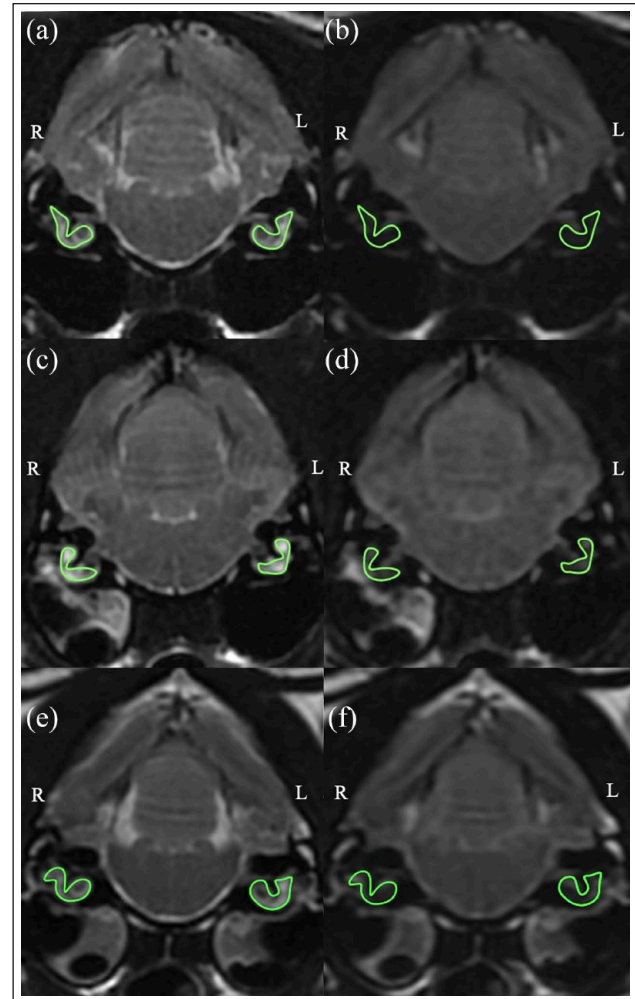


**Figure 1** MRI with regions of interests delineated using Horos. (a) Transverse T2-weighted (T2W) image at the level of the bullae in a cat with normal MRI findings. (b) Transverse fluid-attenuated inversion recovery (FLAIR) image at the level of the bullae in a cat with normal MRI findings. (c) Transverse T2W image at the level of the bullae in a cat with presumptive right-sided otitis media/interna (OMI). (d) Transverse FLAIR image at the level of the bullae in a cat with presumptive right-sided OMI. (e) Transverse T2W image at the level of the bullae in a cat with bilateral OMI. (f) Transverse FLAIR image at the level of the bullae in a cat with bilateral OMI

Any remaining comparisons were tested for normality using Kolmogorov–Smirnov, Cramer–von Mises and Shapiro–Wilk tests. Where any data did not meet the assumptions of normality, they were log-transformed. Post-hoc Tukey tests were then performed to make pairwise comparisons, with a *P* value set at <0.05.

## Results

A total of 41 cats met the inclusion criteria, six with OMI (group A), eight in the inflammatory group (group B), 14 in the non-inflammatory structural brain abnormality group (group C) and 13 in the control group (group D).

**Table 1** Group, signalment and presumptive diagnosis for each cat

| Group | Breed | Sex | Age (years) | Presumptive diagnosis |
|---|---|---|---|---|
| A | Oriental Shorthair | FI | 1 | Bilateral OMI |
| A | DSH | MC | 16 | Bilateral OMI |
| A | DSH | FS | 2 | Left otitis interna, suspected left ear polyp between horizontal external ear canal and dorsolateral compartment of middle ear, OMI |
| A | DSH | MC | 8 | Right OMI, lymphocytic meningoencephalitis |
| A | DSH | MC | 11 | Bilateral OMI |
| A | DSH | FS | 11 | Left OMI + bulla osteitis + left encephalopathy (suspected secondary to otitis) – confirmed by cytology |
| B | DSH | MC | 9 | Suspected FIP |
| B | DSH | FS | 10 months | Suspected infectious meningoencephalitis |
| B | DLH | FS | 8 | Ependymitis + masticatory muscle myositis |
| B | DSH | MC | 2 | Suspected *Cuterebra* myiasis + secondary meningoencephalitis |
| B | Egyptian Mau | MC | 11 | Confirmed meningoencephalitis and ependymitis |
| B | DSH | MC | 7 | Suspected infectious meningoencephalitis |
| B | Angora | MC | 5 months | Suspected FIP |
| B | DSH | MC | 6 | Suspected infectious meningoencephalitis |
| C | DSH | FS | 10 | Left olfactory lobe extra-axial mass |
| C | DSH | FS | 6 | Intracranial, extra-axial mass centered on the falx cerebri |
| C | Norwegian Forest Cat | FS | 6 | Third ventricular mass |
| C | DSH | FS | 14 | Intra-axial mass at the level of the left thalamus |
| C | DSH | FS | 10 | Extra-axial mass, transforaminal herniation |
| C | Devon Rex | FS | 15 | Basisphenoid bone mass |
| C | DSH | FS | 14 | Extra-axial mass, right frontoparietal cortex |
| C | DSH | FS | 14 | Intraventricular meningioma |
| C | DSH | FS | 14 | Lymphoma – right parietal bone + adjacent meninges |
| C | DSH | FS | 17 | Ischemic CVA, left caudal cerebellum and right medulla oblongata |
| C | DLH | MC | 9 | Suspected right middle cerebral artery infarct |
| C | DSH | FS | 14 | Ischemic CVA, left cerebrum (left thalamus, internal capsule + caudate nucleus). Comorbidities: hyperthyroidism, gastrointestinal lymphoma |
| C | DSH | MC | 5 | Suspected right middle cerebral artery infarct |
| C | Siamese | MC | 2 | Porencephaly |
| D | DSH | MC | 8 | Idiopathic epilepsy (tier II) |
| D | Ragdoll | FS | 5 | Idiopathic epilepsy (tier II) |
| D | DLH | MC | 3 | Idiopathic epilepsy (tier II) |
| D | DLH | MC | 11 | Idiopathic epilepsy (tier II) |
| D | DSH | FS | 3 | Suspected movement disorder – fly catching |
| D | DSH | MC | 6 | Idiopathic epilepsy (tier II) |
| D | DLH | FS | 2 | Idiopathic epilepsy (tier II) |
| D | DSH | MC | 14 | Pancreatitis, behavioral changes |
| D | DSH | MC | 2 | Idiopathic epilepsy (tier II) |
| D | Ragdoll | FI | 2 months | Traumatic cervical myelopathy |
| D | DSH | MC | 14 | Blindness – suspected primary ophthalmological disease |
| D | Sphynx | MC | 7 | Suspected movement disorder |
| D | DSH | MC | 1 | T5 vertebral angiomatosis |

FI = female intact; OMI = otitis media/interna; DSH = domestic shorthair; MC = male castrated; FS = female spayed; FIP = feline infectious peritonitis; DLH = domestic longhair; CVA = cerebrovascular accident

Patient signalments for each group are provided in Table 1. Group B contained three cats with suspected infectious meningoencephalitis, two cats with suspected FIP, one with ependymitis and myositis of the masticatory muscles (suspected to be autoimmune rather than infectious based on response to treatment), one with ependymitis

and meningoencephalitis, and one with suspected *Cuterebra* myiasis with secondary meningoencephalitis. The non-inflammatory structural group (group C) included nine cats with intracranial neoplasms, four cats with cerebrovascular accidents and one cat with porencephaly. The control group (group D) included seven cats with idiopathic epilepsy (with structural causes for seizures ruled out by brain MRI and CSF analysis), two cats with paroxysmal episodes, one cat with pancreatitis and questionable behavioral changes, one cat with blindness, one cat with traumatic cervical myelopathy and one cat with thoracic vertebral angiomatosis. In all the groups there appeared to be only one cat with concurrent non-clinical, unilateral, left OMI. This was a cat in the non-inflammatory structural disease group (group C) that had a right middle cerebral artery infarct.

The mean FLAIR suppression ratio, CSF nucleated cell count and CSF protein concentrations for each group are provided in Table 2. The mean FLAIR suppression ratio of group A was significantly lower than that of group B ($P <0.001$), group C ($P = 0.0046$) and group D ($P <0.001$). There was no significant difference in FLAIR suppression ratio between any of the other groups included in the study (Figure 2). Unexpectedly, female entire cats appeared to have significantly lower FLAIR suppression ratios compared with female spayed and male castrated cats.

Mean CSF cell count was significantly higher in the OMI group (group A) compared with the control group (group D; $P = 0.0039$). CSF cell count in the inflammatory group (group B) was also statistically significantly higher

**Table 2** Mean fluid-attenuated inversion recovery (FLAIR) suppression ratio, cerebrospinal fluid (CSF) nucleated cell count and CSF protein concentration in each group

| Group | Mean FLAIR suppression ratio | Mean CSF nucleated cell count ($\times 10^9$/l) | Mean CSF protein concentration (g/l) |
|-------|------------------------------|-------------------------------------------------|--------------------------------------|
| A | 0.6249 | 0.016 | 0.132 |
| B | 0.7599 | 0.007 | 0.627 |
| C | 0.7138 | 0.003 | 0.702 |
| D | 0.7490 | 0.0008 | 0.083 |

than in the control group (group D; $P = 0.0009$). There was no other significant difference between groups; however, there was a statistically significant positive correlation between age and nucleated cell count ($P = 0.01$; Figure 3).

CSF protein concentration was statistically significantly higher in the inflammatory group (group B) compared with the OMI group (group A; $P = 0.02$) and the control group (group D; $P = 0.0001$). The non-inflammatory structural group (group C) also had a statistically significantly higher mean protein concentration compared with the OMI group (group A; $P = 0.027$) and the control group ($P = 0.0009$). There was no statistically significant difference between any of the other groups (Figure 4).

## Discussion

To our knowledge, there have been no previous studies on the use of MRI FLAIR for the investigation of vestibular disease in cats. This study confirmed that there is a
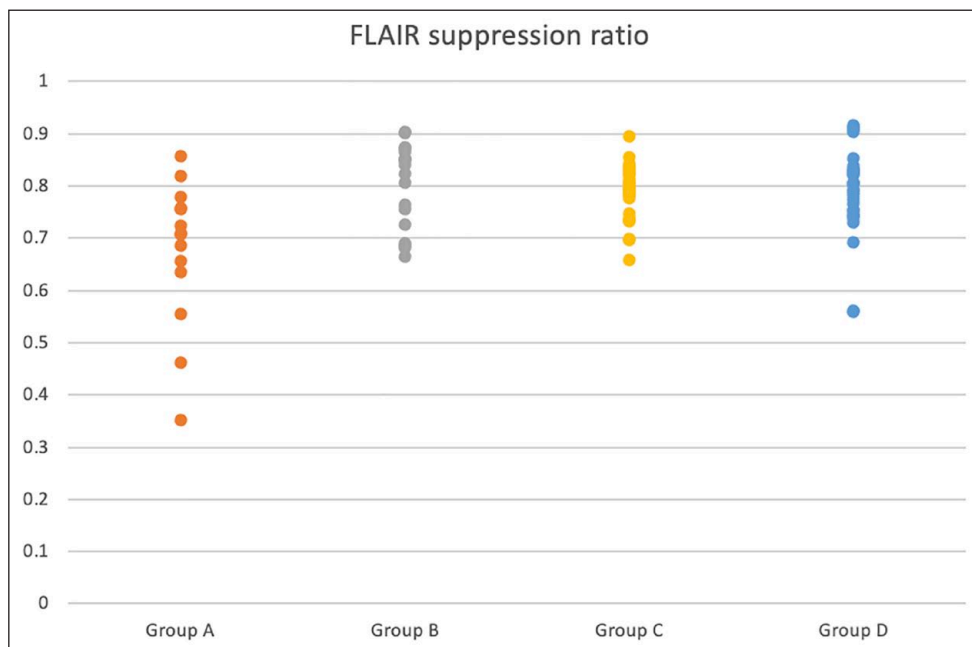


**Figure 2** Dot plot showing the distribution of fluid-attenuated inversion recovery (FLAIR) suppression ratio in each group
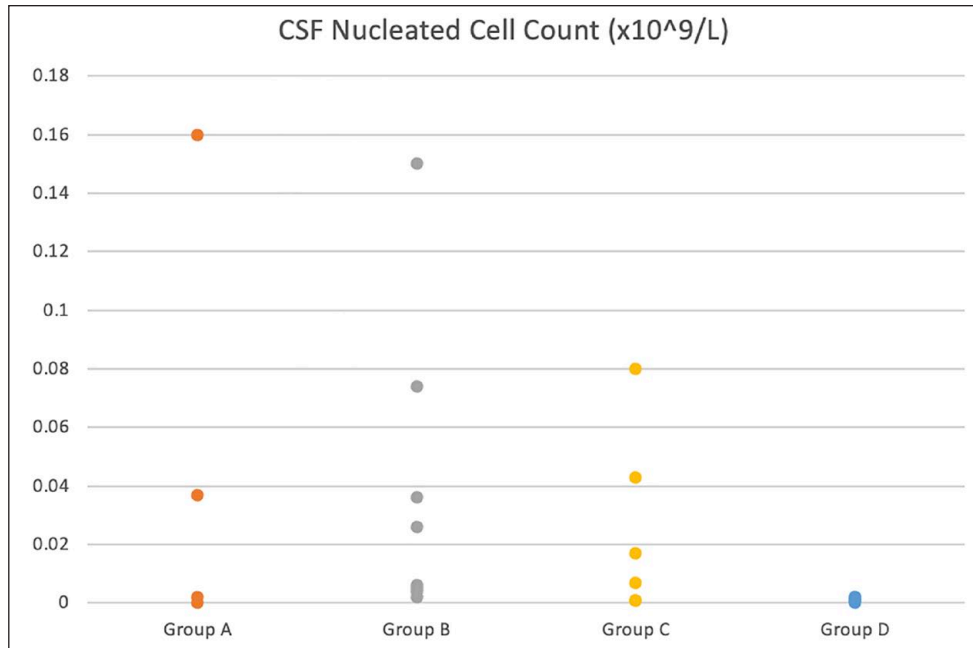
**Figure 3** Dot plot showing the distribution of nucleated cell count in the cerebrospinal fluid (CSF) of cats in each group
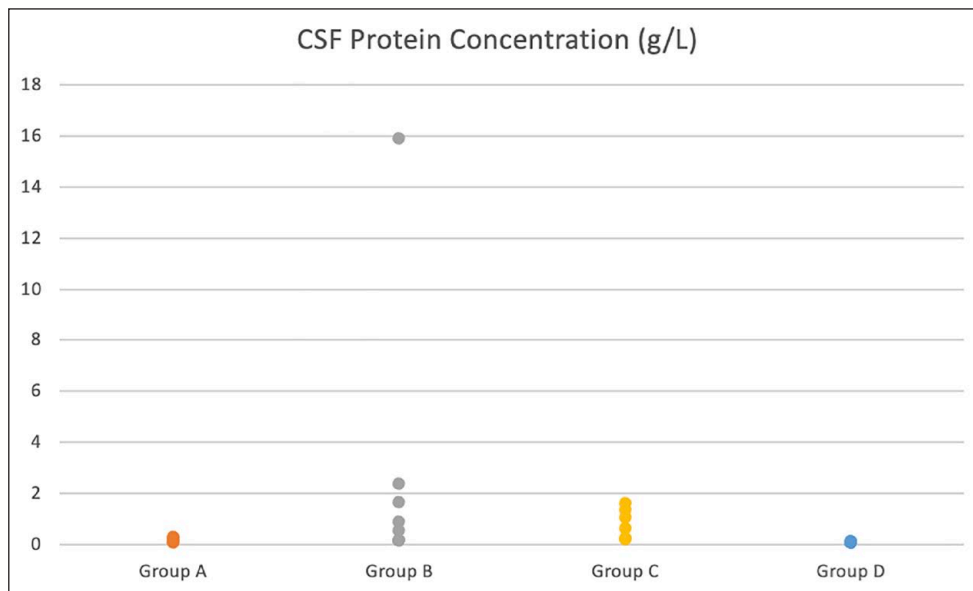


**Figure 4** Dot plot showing the distribution of cerebrospinal fluid (CSF) protein concentration in each group

significantly lower FLAIR suppression ratio in the inner ears of cats with OMI (counting both affected and unaffected ears) compared with cats with other pathologies. The results also demonstrated a significantly increased CSF nucleated cell count in the cats with OMI and those with inflammatory brain disease (group B). There were also significantly increased CSF protein levels in cats with inflammatory brain disease (group B) compared with the control group (group D) and cats with OMI (group A). The cats with non-inflammatory structural brain disease

(group C) also had significantly higher CSF protein concentrations than the control and OMI group.

The utility of MRI in diagnosing inner ear disease has previously been documented in humans. Inflammation of the middle and inner ear leads to breakdown of the blood–perilymph barrier. This causes altered composition of the perilymph, more specifically an influx of inflammatory cells and proteins.[7,9,14] Typically, normal CSF suppresses on MRI FLAIR sequences, whereas inflammatory conditions, such as meningitis, have been shown

to reduce FLAIR suppression vs T2W sequences.[15–17] Additionally, a 10–15-fold increase in the protein content of perilymph in humans with schwannomas undergoing labyrinth taps has been reported.[11,12,18] Given that normal perilymph communicates with, and is very similar in composition to, normal CSF, this should theoretically also show less suppression on FLAIR sequences compared with the contents of normal inner and middle ears. The diagnostic utility of this has previously been demonstrated in humans, in differentiating between primary and secondary inner ear disease using three-dimensional FLAIR, as well as enabling the identification of haemorrhage or increased protein.[19]

To our knowledge, the potential of FLAIR MRI in diagnosing inner ear disease in veterinary patients (dogs) was first demonstrated by Castillo et al.[13] They found that the affected ears in dogs with OMI had a significantly lower FLAIR suppression ratio compared with unaffected ears. Our study confirmed that the inner ear FLAIR suppression ratio was also significantly lower in cats with presumptive OMI compared with cats with other CNS conditions. As this was a smaller study and most of the affected cats had bilateral OMI, the affected ear could not be compared to the unaffected side. Therefore, the FLAIR suppression ratio in both ears (whether affected or not) was included when calculating the mean suppression ratio. Despite the results potentially being skewed by this, the inner ear FLAIR suppression ratio in group A was still significantly lower than in all other groups. Female entire cats had a significantly lower FLAIR suppression ratio than all other sexes. It is suspected that this was a statistical issue, as only 2/41 cats in the study were female, one of which had bilateral OMI.

The significantly increased CSF nucleated cell count in the OMI group compared with the control group was expected, contrary to the results of the study performed by Castillo et al,[13] which did not find a correlation between lack of inner ear FLAIR suppression and pleocytosis in dogs. As patients were included in group A if they were clinical for OMI (ie, neurological examination localized to the peripheral vestibular system), consistent with findings on MRI, this included patients that may have had meningitis secondary to otogenic infection. As the sample size for this study was very small, these results may have been skewed by a small number of outliers (ie, cats with both OMI and meningitis). In order to determine whether CSF nucleated cell count is truly elevated in cats with OMI, a larger study to account for outliers would be useful. Age being significantly associated with an increased CSF nucleated cell count could suggest that older age in cats is associated with intracranial, structural causes of neurological signs rather than idiopathic conditions. For example, it has previously been shown that younger cats are significantly more likely to have idiopathic epilepsy than structural epilepsy.[20,21] Interestingly, this is in contrast to a recent study that investigated MRI findings in dogs presenting to a single center, where it was found that there was a significant negative correlation between age and the incidence of asymmetric encephalopathy or meningoencephalopathy.[22] This may be due to the relatively low prevalence of meningoencephalitis of unknown origin in cats vs dogs.[23]

The CSF protein concentration was significantly higher in the inflammatory disease group (group B) and the non-inflammatory structural disease group (group C) than in the OMI group (group A) and the control group (group D). This was expected in cats with inflammatory disease vs those without. In humans, elevated CSF total protein concentrations have been associated with a number of conditions.[24,25] Additionally, one study in cats revealed moderate-to-markedly elevated CSF total protein concentrations only in patients with FIP, suggesting that the inclusion of cats with FIP in the inflammatory group may have influenced the CSF total protein concentration for the group.[26] Interestingly, despite the nucleated cell count in the OMI group (group A) being significantly higher compared with the control group (group D), the protein concentration was not. The fact that the non-inflammatory structural disease group (group C) had a significantly higher CSF protein concentration, but not nucleated cell count, compared with the OMI group (group A) and control group (group D), may suggest a higher incidence of albuminocytologic dissociation in this group vs the inflammatory disease group (group B).

A major weakness of this study was the small sample size. This meant that results for FLAIR suppression, as well as CSF nucleated cell count and protein concentrations, could easily be skewed by any outliers. There was a particularly small sample size for cats with a working diagnosis of OMI. For this reason, diagnosis was confirmed by cytology in only 1/6 cats, meaning 5/6 cats in group A had a presumptive diagnosis based on MRI and CSF findings as well as response to treatment. A larger study with cytology and culture performed on middle ear content from all cats suspected to have OMI based on imaging findings would improve the reliability of the results. Finally, this was also a retrospective study, meaning there were variables that could not be controlled for, including time between presentation and MRI being performed.

## Conclusions

This study demonstrates the potential diagnostic utility of MRI FLAIR sequences in diagnosing presumptive OMI in cats, similarly to in humans and dogs. This makes this study relevant to practicing veterinary neurologists and radiologists in interpreting MRI findings in cats with suspected OMI. A larger, prospective study investigating differences in FLAIR suppression ratio between the affected and unaffected ears in cats with OMI would further

confirm our ability to distinguish between the affected and unaffected ears using MRI FLAIR sequences. This would also help to determine whether CSF nucleated cell count in cats with OMI is truly elevated compared with normal cats, or whether the results of this study were skewed by a few outliers with secondary inflammatory disease.

**ORCID iD** Stephen Everest (iD) https://orcid.org/0000-0003-2778-8363

## References

1 Grapes NJ, Taylor-Brown FE, Volk HA, et al. **Clinical reasoning in feline vestibular syndrome: which presenting features are the most important?** *J Feline Med Surg* 2021; 23: 669–678.

2 DeLahunta A, Glass E and Kent M. **Vestibular system: special proproception.** In: DeLahunta A, Glass E and Kent M (eds). De Lahunta's veterinary neuroanatomy and clinical neurology. Philadelphia, PA: Elsevier, 2021, pp 345–373.

3 Uemura EE. **Vestibular system.** In: Uemura EE (ed). Fundamentals of canine neuroanatomy and neurophysiology. New York, NY: Wiley-Blackwell, 2015, pp 307–328.

4 Naganawa S, Satake H, Iwano S, et al. **Communication between cochlear perilymph and cerebrospinal fluid through the cochlear modiolus visualized after intratympanic administration of Gd-DTPA.** *Radiat Med* 2008; 26: 597–602.

5 Reinbacher E, Kneissl S, Hirt R, et al. **Myringotomy in dogs: contamination rate from the external ear canal – a pilot study.** *Vet Anim Sci* 2020; 10: 100125. DOI: 10.1016/j.vas.2020.100125.

6 Thomsen J, Saxtrup O and Tos M. **Quantitated determination of proteins in perilymph in patients with acoustic neuromas.** *J Otorhinolaryngol Relat Spec* 1982; 44: 61–65.

7 Hirose K and Li SZ. **The role of monocytes and macrophages in the dynamic permeability of the blood-perilymph barrier.** *Hear Res* 2019; 374: 49–57.

8 Rasmussen JE, Ran Laurell G, Rask-Andersen H, et al. **The proteome of perilymph in patients with vestibular schwannoma. A possibility to identify biomarkers for tumor associated hearing loss?** *PLoS One* 2018; 13. DOI: 10.1371/journal.pone.0198442.

9 Lin HC, Renid Y, Lysaght AC, et al. **Proteome of normal human perilymph and perilymph from people with disabling vertigo.** *PLoS One* 2019; 14. DOI: 10.1371/journal.pone.0218292.

10 Kim TY, Park DW, Lee YJ, et al. **Comparison of inner ear contrast enhancement among patients with unilateral inner ear symptoms in MR images obtained 10 minutes and 4 hours after gadolinium injection.** *Am J Neuroradiol* 2015; 36: 2367–2372.

11 Petrovic BD, Futterer SF, Hijaz T, et al. **Frequency and diagnostic utility of intralabyrinthine FLAIR hyperintensity in the evaluation of internal auditory canal and inner ear pathology.** *Acad Radiol* 2010; 17: 992–1000.

12 Bhadelia RA, Tedesco KL, Hwang S, et al. **Increased cochlear fluid-attenuated inversion recovery signal in patients with vestibular schwannoma.** *Am J Neuroradiol* 2008; 29: 720–723.

13 Castillo G, Parmentier T, Monteith G, et al. **Inner ear fluid-attenuated inversion recovery MRI signal intensity in dogs with vestibular disease.** *Vet Radiol Ultrasound* 2020; 61: 531–539.

14 de Risio L, Bhatti S, Muñana K, et al. **International veterinary epilepsy task force consensus proposal: diagnostic approach to epilepsy in dogs.** *BMC Vet Res* 2015; 11: 148. DOI: 10.1186/s12917-015-0462-1.

15 Hamza Kamr W, Eissawy MG and Saadawy A. **The value of contrast-enhanced FLAIR magnetic resonance imaging in detecting meningeal abnormalities in suspected cases of meningitis compared to conventional contrast-enhanced T1WI sequences.** *Egypt J Radiol Neurol Nuclear Med* 2020; 51: 231. DOI: 10.1186/s43055-020-00348-2.

16 Bangerter NK, Hargreaves BA, Gold GE, et al. **Fluid-attenuated inversion-recovery SSFP imaging.** *J Magn Reson Imaging* 2006; 24: 1426–1431.

17 Okuda T, Korogi Y, Shigematsu Y, et al. **Brain lesions: when should fluid-attenuated inversion-recovery sequences be used in MR evaluation?** *Radiology* 1999; 212: 793–798.

18 Lee IH, Kim HJ, Chung WH, et al. **Signal intensity change of the labyrinth in patients with surgically confirmed or radiologically diagnosed vestibular schwannoma on isotropic 3D fluid-attenuated inversion recovery MR imaging at 3 T.** *Eur Radiol* 2010; 20: 949–957.

19 Sugiura M, Naganawa S, Teranishi M, et al. **Three-dimensional fluid-attenuated inversion recovery magnetic resonance imaging findings in patients with sudden sensorineural hearing loss.** *Laryngoscope* 2006; 116: 1451–1454.

20  Pákozdy Á, Leschnik M, Sarchahi AA, et al. **Clinical comparison of primary versus secondary epilepsy in 125 cats.** *J Feline Med Surg* 2010; 12: 910–916.

21  Schriefl S, Steinberg TA, Matiasek K, et al. **Etiologic classification of seizures, signalment, clinical signs, and outcome in cats with seizure disorders: 91 cases (2000–2004).** *J Am Vet Med Assoc* 2008; 233: 1591–1597.

22  Walsh N, Carney PC, Streu S, et al. **Prevalence of brain magnetic resonance imaging diagnoses and correlation with signalment and presenting complaint in dogs.** *Front Vet Sci* 2021; 8: 1349. DOI: 10.3389/fvets.2021.768709.

23  Nessler J, Wohlsein P, Junginger J, et al. **Meningoencephalomyelitis of unknown origin in cats: a case series describing clinical and pathological findings.** *Front Vet Sci* 2020; 7: 291. DOI: 10.3389/fvets.2020.00291.

24  Matsuo T. **Vestibular neuronitis—serum and CSF virus antibody titer.** *Auris Nasus Larynx* 1986; 13: 11–34.

25  Brooks JA, McCudden C, Breiner A, et al. **Causes of albuminocytological dissociation and the impact of age-adjusted cerebrospinal fluid protein reference intervals: a retrospective chart review of 2627 samples collected at tertiary care centre.** *BMJ Open* 2019; 9. DOI: 10.1136/bmjopen-2018-025348.

26  Singh M, Foster DJ, Child G, et al. **Inflammatory cerebrospinal fluid analysis in cats: clinical diagnosis and outcome.** *J Feline Med Surg* 2005; 7: 77–93.